

Dye-sensitized Solar Cell utilizing Gold Doped Reduced Graphene Oxide Films Counter Electrode

M.Y.A. Rahman*, A.S. Sulaiman and A.A. Umar

Institute of Microengineering and Nanoelectronics (IMEN), Universiti Kebangsaan Malaysia, 43600, Bangi, Selangor, Malaysia

Received: October 02, 2017, Accepted: March 07, 2018, Available online: May 02, 2018

Abstract: This work is concerned with the use of gold doped reduced graphene oxide (rGO) films as counter electrode in a dye-sensitized solar cell (DSSC). The effect of gold content on the photovoltaic parameters of the device has been studied. The samples are crystalline, indicated by the presence of rGO phase. It was found that the short-circuit current density (J_{sc}) decreases with the increase in gold content. The DSSC utilizing the sample prepared using 2.0 wt.% gold demonstrated the highest J_{sc} , V_{oc} and η of 0.989 mA cm⁻², 0.692 V and 0.175%, respectively. The highest efficiency (η) of the device is due to the lowest leak current and charge transfer resistance (R_{ct}).

Keywords: counter electrode, dye-sensitized solar cell, doping, gold, graphene oxide

1. INTRODUCTION

The role of counter electrode in DSSC is to serve as a medium to receive electrons from external circuit for reducing oxidizing species to reducing species such as triiodide to iodide. Platinum films have widely been utilized as counter electrode in DSSC since it is the most electrochemically stable metal against the redox couple of iodide/triiodide in liquid electrolyte. However, the main limitation of platinum is costly material, making it is unsuitable for large scale DSSC production. The research on replacing platinum film counter electrode in DSSC with much cheaper material has actively been investigated. The use of carbon film as counter electrode in DSSC has been attempted by several researchers since it has high electronic conductivity, corrosion resistance, electrochemical reactivity and low cost [1-3]. Graphite film has been utilized as counter electrode in a solid state photo-electrochemical cell (PEC) since it is much cheaper than platinum and can be prepared in film form via electron beam evaporation technique [4].

Another material that can replace platinum as counter electrode in DSSC is graphene. Graphene is a two-dimensional carbon sheet has attracted great interest due to its unique properties to be applied as counter electrode in DSSC [5]. Several researchers have utilized graphene films as counter electrode in DSSC [5-11]. It was found that the power conversion efficiency of the DSSC utilizing graphene films counter electrode was comparable with that using platinum films counter electrode [5-11]. In our previous

work, we have utilized reduced graphene oxide as counter electrode in DSSC and achieved a low efficiency of 0.09% [12].

Since the efficiency is low, the electrical property of rGO should be improved by doping it with metallic material and consequently improves the efficiency of the device. The idea of doping of RGO with metal has been attempted by Soo et al. 2016 who doped silver into rGO films for use as a catalyst in fuel cell [13]. Xue et al. 2012 utilized nitrogen doped graphene foams as counter electrode in DSSC [14]. Ju et al. 2013 used nitrogen doped graphene nanoplatelets as superior metal free counter electrode for DSSC [15]. Wang et al. 2014 utilized phosphorous doped reduced graphene oxide (rGO) an electrocatalyst counter electrode in DSSC [16].

In this work, we have doped rGO with gold in order to improve the electronic conductivity of RGO films. Gold doped reduced graphene oxide (rGO) films was then utilized as a counter electrode in DSSC. The originality of this work is the use of gold doped rGO films as counter electrode of DSSC. The goal of this work is to investigate the effect of gold content in term of its percentage by weight on the performance parameters of the DSSC. These parameters were then linked with leak current and EIS data such as R_b , R_{ct} and carrier lifetime.

2. EXPERIMENTAL

2.1. Preparation and characterization of gold doped rGO

Firstly, 0.1 g GO powders were dissolved in 50 ml deionized water. The solution was then sonicated for 1 h. Then, 2 mg gold

*To whom correspondence should be addressed: Email: mohd.yusri@ukm.edu.my
Phone: 60389118543, Fax.: 60389250439

(III) chloride trihydrate ($\text{HAuCl}_3 \cdot 3\text{H}_2\text{O}$) powder was then added into the solution and sonicated for 30 minutes and stirred for 5 minutes. 2 mg is equivalent to 2 wt.%. The solution was spin coated 3 times on ITO substrate at 1000 rpm for 15 s. The sample was annealed at 100°C in argon atmosphere for 15 minutes. These procedures were repeated by dissolving 2.5, 3.0, 3.5 and 4.0 wt.% $\text{HAuCl}_3 \cdot 3\text{H}_2\text{O}$, corresponding with 2.5, 3.0, 3.5 and 4.0 mg $\text{HAuCl}_3 \cdot 3\text{H}_2\text{O}$ powder respectively into 50 ml deionized water. The structure of the samples was characterized by using Bruker D8 Advanced x-ray diffractometer with CuK radiation at a scan rate of $0.025^\circ/0.1$ s. The transmission of the samples was studied by UV-Vis spectrometer.

2.2. Fabrication and performance study of DSSC

The DSSC consisting of TiO_2 films as photoanode and gold doped rGO film as counter electrode was fabricated. The TiO_2 films were prepared on ITO substrate via liquid phase deposition technique at the growth temperature of 40°C . 0.5 M $\text{LiI}/0.05$ M $\text{I}_2/0.5$ M TBP in acetonitrile was used as an electrolyte containing iodide/triiodide redox couple. A DSSC was fabricated by sandwiching the parafilm between TiO_2 film and gold doped rGO electrode film. The structure was clamped in order to optimize the contact of the components of the cell. The electrolyte was injected into the structure via a capillary. The current-voltage curves in dark and under illumination were recorded by a Keithley high-voltage source model 237 interfaced with a personal computer. The photovoltaic performance of the DSSC utilizing gold doped rGO films counter electrode with various gold contents was investigated by current-voltage measurement under 100 mW cm^{-2} tungsten light using Keithley 237 source measurement unit. The illuminated area of the device was 0.23 cm^2 . The electrochemical impedance spectroscopy (EIS) technique was also performed to study the bulk resistance (R_b), the charge interfacial resistance (R_{ct}) and charge carrier lifetime at the applied voltage of 0.4 V.

3. RESULTS AND DISCUSSION

Fig. 1 depicts the XPS spectra for the Au-doped rGO with various gold concentrations. The spectra show that the presence of the peak of Au 4f, C 1s and O 1s. The location of binding energy for each peak is illustrated in Table 1. The presence of short peak of Au indicates that its atoms are incorporated into rGO with small amount due to small amount of its doping into rGO lattice that is only 1-4 wt.%. The C 1s and O 1s peaks signify the presence of oxygen functional groups such as C-O bonds, carbonyls or carboxylates on GO [16]. From the table, it is found that the binding energy position of Au 4f decreases with Au content until the 2% wt. Au, then increases at 3% wt. and finally drops again at 4% wt. Au. This trend is not observed for C 1s and O 1s. For C 1s, the binding energy position decreases with Au concentration until 3 % wt. Au and then increases at 4 %wt. Au. However, for O 1s, its binding energy position increases with gold content in the whole range of % wt. Au as illustrated in the table.

Fig. 2 shows the XRD spectra of gold doped rGO films with various contents of gold. The spectra only demonstrates one dominant peak of rGO at the crystal plane (002) corresponding with the diffraction angle of 10.5° for all samples. This result is consistent with that reported in [17]. The 3.5 wt.% sample possesses the highest peak intensity while the 4.0 wt.% sample shows the lowest peak intensity. All samples except 4.0 wt.% sample have the peak at

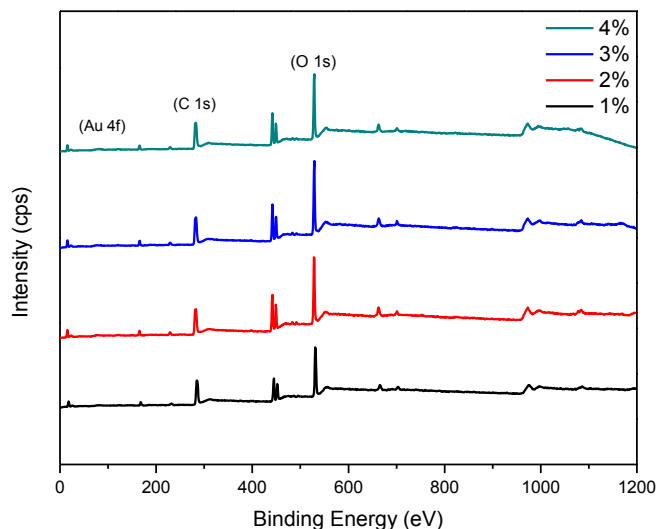


Figure 1. XPS spectra of gold doped rGO with various gold contents

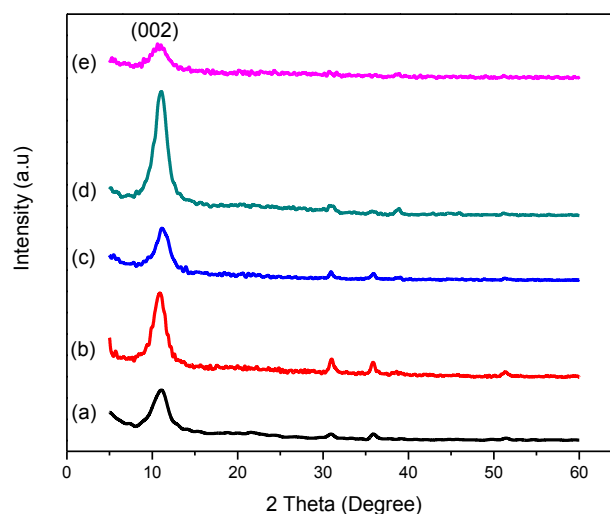


Figure 2. XRD patterns of gold doped rGO film sample, (a) 2.0, (b) 2.5, (c) 3.0, (d) 3.5 and (e) 4.0 wt.% gold

31.3 and 35.5° corresponding with (111) and (200) planes, respectively. These peaks belong to ITO substrate. This result agrees well with that reported in [18]. The peak of gold is not detected in the XRD pattern for each sample, confirming that gold has successfully been doped into rGO lattice. This is due to the amount of gold that

Table 1. Position of binding energy for Au, C and O peak with various gold contents

| % wt. | Au 4f (eV) | C 1s (eV) | O 1s (eV) |
|-------|------------|-----------|-----------|
| 1 | 81.512 | 289.061 | 531.012 |
| 2 | 80.894 | 287.194 | 531.594 |
| 3 | 95.200 | 285.000 | 533.300 |
| 4 | 81.000 | 289.150 | 536.600 |

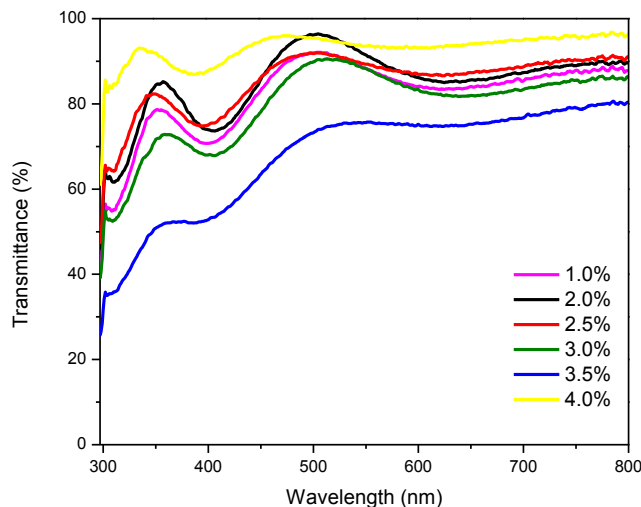


Figure 3. UV-Vis transmission spectra of gold doped RGO film sample with various wt.% gold

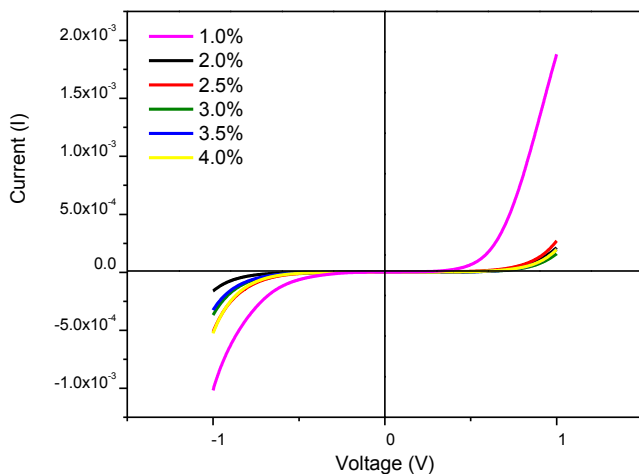


Figure 4. I - V curves of the devices in dark with various gold contents

was doped into the lattice of rGO is so small which is in the range 2.0-4.0 wt.%. From the spectra, the full width half maximum at (002) for each sample is determined and from which the crystallite size is computed from the Scherer formula and illustrated in Table 2. From the table, it is noticed that the crystallite size increases from 2.0 to 3.0 wt.% and then drops.

Fig. 3 depicts the UV-Vis transmission spectra of gold doped

Table 2. FWHM and crystallite size of rGO with various gold contents

| wt.% | FWHM | Crystallite size (Å) |
|------|------|----------------------|
| 2.0 | 1.95 | 40.34 |
| 2.5 | 1.53 | 49.15 |
| 3.0 | 1.63 | 50.90 |
| 3.5 | 1.59 | 49.18 |
| 4.0 | 1.94 | 44.40 |

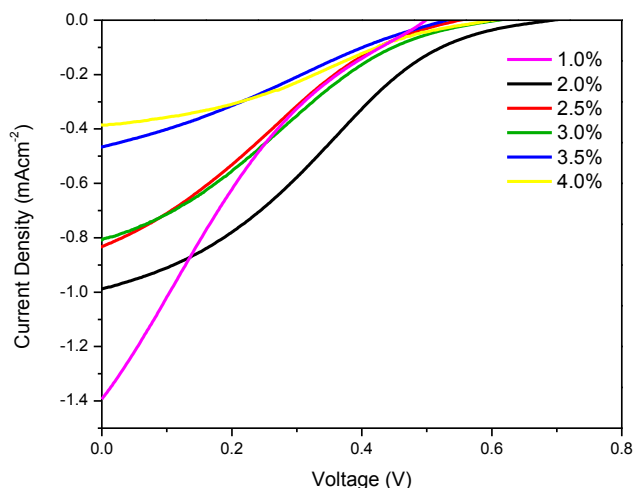


Figure 5. J - V curves of the devices with various gold contents under illumination of 100 mW cm^{-2}

rGO film sample with various gold contents. It is noticed from the spectra that the transmission area varies with the gold content. The 3.5 wt.% sample shows the smallest area of light transmission followed by 3.0, 1.0, 2.5, 2.0 and 4.0 wt.% samples. All samples possess the lowest transmission in UV region and highest transmission in visible region in the region 400-700 nm. It is found that the transmission in IR region with the wavelength above 700 nm is higher than that in UV region with the wavelength below 400 nm.

Fig. 4 shows the I - V curves in dark of the DSSCs utilizing gold doped rGO films counter electrodes with various wt.% gold. It is noticed that the devices do not show diode property since the dark current in reverse bias is slightly larger than that in forward bias. The dark current in reverse bias is also called leak current. The different in the leak current is quite significant indicating that the content of gold affects the leak current. However, the difference in dark current in forward bias is small, signifying that the gold content does not influence the forward bias dark current. The device utilizing 2.0 wt.% gold possesses the lowest leak current followed by 3.5, 3.0, 4.0, 2.5 and 1.0 wt.% samples.

Fig. 5 shows the current density-voltage (J - V) curves of the DSSC utilizing the samples prepared with various gold contents under 100 mW cm^{-2} light illuminations. The device with 4.0 wt.% gold shows the lowest output power, followed by 3.5, 2.5, 3.0, 1.0 and 2.0 wt.% samples. The curves have high slope, indicating that high internal resistance of the devices leading to high output power loss which is also due to high leak current as shown in Fig. 4. Such shape of the curve has also been reported by Choi et al. 2011 who studied the DSSC utilizing graphene based carbon nanotubes composite counter electrode [19]. Rahman et al. 2016 also reported the same shape of the J - V curves obtained from the DSSC utilizing rGO counter electrode [12]. High power loss also resulted in low fill factor (FF) and power conversion efficiency (η) as illustrated in Table 1. The other photovoltaic parameters are extracted from Fig. 5 and illustrated in Table 2.

Fig. 6 shows Nyquist plots of the DSSC utilizing gold doped rGO films counter electrode prepared at various gold contents.

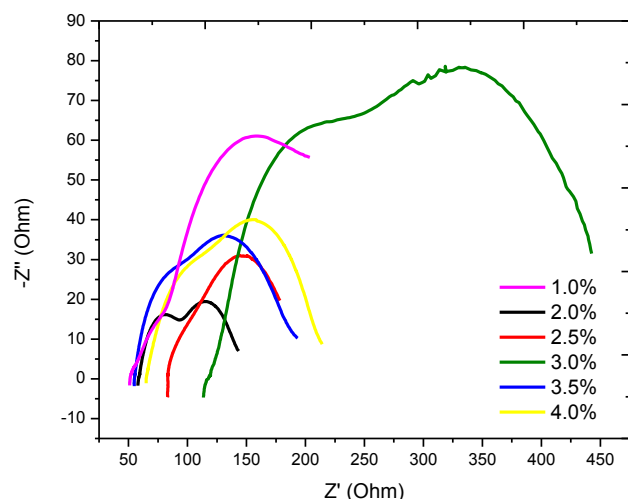


Figure 6. Nyquist plots of the DSSCs utilizing gold doped RGO films counter electrode prepared at various gold contents.

From the plots, two resistances are obtained, namely, bulk resistance (R_b) of the device represented by smaller semicircle and charge transfer resistance (R_{ct}) represented by bigger semicircle. However, these two semicircles are not clearly seen in the plots since they overlap. The bulk resistance is contributed by the resistance of each component of the device. The charge transfer resistance is attributed by the resistance at the interface of $\text{TiO}_2\text{-N719}$ /electrolyte and electrolyte/gold doped rGO. Both resistances are presented in Table 2. From Table 2, it is found that R_{ct} is always higher than R_b for each device. It is found that the device with 2.5 wt.% gold possesses the lowest R_b followed by 2.0, 1.0, 3.5, 4.0 and 3.0 wt.% samples. However, the device with 2.0 wt.% gold has the lowest R_{ct} , followed by 2.5, 4.0, 3.5, 4.0 and 1.0 wt.% samples.

Fig. 7 depicts the Bode plots of the devices utilizing gold doped rGO film counter electrode prepared with various gold contents. It was found that there is one peak appears in the Bode spectra. The peak represents the resonant frequency for each device. The carrier lifetime was calculated from the frequency and illustrated in Table 1. According to the table, the 2.0 wt.% sample possesses the shortest lifetime, followed by 3.5, 4.0, 3.0, 2.5 and 1.0 wt.% samples.

Table 3 illustrates the photovoltaic parameters, R_b , R_{ct} and carrier lifetime with various gold contents. According to the table, it was found that the device with 2.0 wt.% gold performs the highest J_{SC} , V_{OC} and η . This is due to the DSSC utilizing 2.0 wt.% sample possesses the smallest leak current depicted in Fig. 3 and the lowest R_{ct} illustrated in Table 2. There is no significant change in V_{OC} . Generally, from Table 2, the FF is low since the area of maximum power

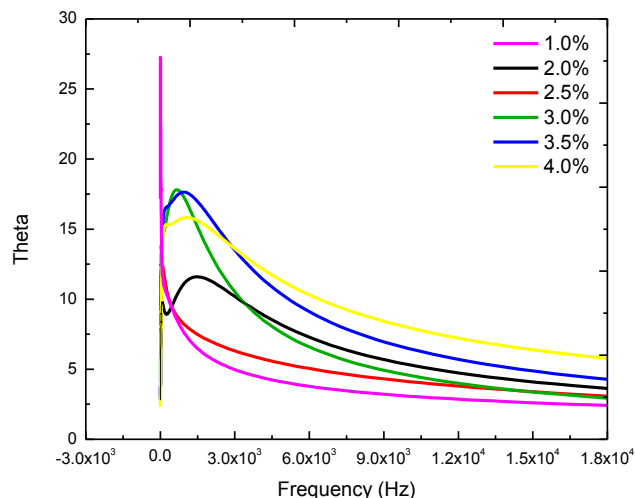


Figure 7. Bode plots of the DSSCs utilizing gold doped RGO films counter electrode prepared at various gold contents

rectangles drawn from the $J-V$ curves is much smaller than that of the $J-V$ curves shown in Fig. 5. According to the observation on the above performance studies of the DSSC, it is concluded that the J_{SC} decreases with the gold content in term of its percentage by weight. There are 4 devices, namely, that with 1.0, 2.0, 2.5 and 3.0 wt.% demonstrate higher efficiency than that of the device utilizing pure rGO counter electrode. However, the η decreases with gold content until the 3.5 wt.% sample and then re-increases. The highest η obtained in this work, 0.175% is much smaller compared with those reported in [14-16] that are 4.99, 6.81 and 7.80%, respectively. This might be caused the internal resistance of the DSSC fabricated in this work is much higher than those reported in [14-16]. However, it is higher than that of the device utilizing pure rGO counter electrode reported in [8] which was 0.09%. This is because the R_b and R_{ct} of the DSSC utilizing gold doped rGO counter electrode from this work are smaller than those reported in [12]. The R_b and R_{ct} of the DSSC utilizing undoped RGO were 65 and 77 Ω , respectively [12]. This is noticed from Table 2 that the R_b and R_{ct} for the device with the highest η were 40 and 69 Ω , respectively. However, it is observed from Table 2 that the device utilizing 3.5 and 4.0 wt.% gold demonstrated lower η than that with pure rGO. This is due to their R_b and R_{ct} are higher than that of pure rGO as illustrated in Table 3. Future work is aimed at improving the efficiency of the DSSC utilizing gold doped RGO films counter electrode by annealing treatment on the sample in order to reduce the resistance at the interface of $\text{TiO}_2\text{-N719}$ /electrolyte and electrolyte/gold doped reduced rGO.

Table 3. Photovoltaic parameters, EIS data and carrier lifetime with various gold contents

| wt. % | J_{SC} (mA cm ⁻²) | V_{OC} (V) | FF | η (%) | R_b (Ω) | R_{ct} (Ω) | Time (s) |
|-------|---------------------------------|--------------|-------------|-------------|--------------------|-----------------------|----------|
| 1.0 | 1.350±0.002 | 0.498±0.002 | 0.171±0.002 | 0.115±0.004 | 60.0 | 170.0 | 0.0367 |
| 2.0 | 0.989±0.002 | 0.692±0.001 | 0.255±0.003 | 0.175±0.008 | 40.0 | 69.0 | 0.0007 |
| 2.5 | 0.835±0.001 | 0.550±0.002 | 0.234±0.002 | 0.108±0.001 | 25.6 | 126.2 | 0.0125 |
| 3.0 | 0.808±0.004 | 0.609±0.004 | 0.231±0.005 | 0.114±0.005 | 179.0 | 250.0 | 0.0015 |
| 3.5 | 0.467±0.002 | 0.530±0.007 | 0.266±0.003 | 0.056±0.005 | 71.8 | 129.8 | 0.0010 |
| 4.0 | 0.386±0.002 | 0.602±0.006 | 0.300±0.002 | 0.070±0.007 | 90.2 | 127.0 | 0.0010 |

4. CONCLUSIONS

Gold doped reduced graphene oxide (rGO) films counter electrode were successfully prepared on ITO substrate and applied in DSSC. The doping of gold into rGO has decreased the resistance of RGO and improves the performance of the DSSC utilizing gold doped rGO counter electrode. The DSSC utilizing the sample prepared using 2.0 wt.% gold demonstrates the highest J_{SC} and η due to the smallest leak current and charge transfer resistance (R_{ct}). The above results indicate that gold doped rGO has potential as counter electrode candidate for replacing costly platinum in DSSC.

5. ACKNOWLEDGMENTS

This work was supported by Universiti Kebangsaan Malaysia (UKM) under research grant DLP 2015-003 and GUP-2016-013.

REFERENCES

- [1] Z. Huang, X. Liu, K. Li, D. Li, Y. Luo, Hong Li, W. Song, L. Chen, Q. Meng, *Electrochem. Commun.*, 9, 596 (2007).
- [2] J.G. Nam, Y.J. Park, B.S. Kim, J.S. Lee, *Scripta Materialia.*, 62, 148 (2010).
- [3] H. Zhu, H. Zeng, V. Subramanian, C. Masarapu, K-H.Hung, B. Wei, *Nanotechnology*, 19, 465204 (5pp) (2008).
- [4] M.Y.A. Rahman, M.M. Salleh, I.A. Talib, M. Yahaya, *Ionics*, 11, 275 (2005).
- [5] J. D. Roy-Mayhew, D.J. Bozym, C. Punckt, I.A. Aksay, *ACS Nano.*, 4, 6203 (2010).
- [6] D.W. Zhang, X.D. Li, H.B. Li, S. Chen, Z. Sun, X.J. Yin, S.M. Huang, *Carbon*, 49, 5382 (2011).
- [7] H. Wang, K. Sun, F. Tao, D. J. Stacchiola, Y.H. Hu, *Angew. Chem. Int. Ed.*, 52, 9210 (2013).
- [8] L. Kavan, *Top Curr. Chem.*, 348, 53 (2014).
- [9] L. Kavan, J.-H. Yum, M. Grätzel, *Electrochim. Acta*, 128, 349 (2014).
- [10] M. Janani, P. Srikrishnarka, S.V. Nair, A.S. Nair, *J. Mater. Chem. A.*, 3, 17914 (2015).
- [11] L. Kavan, P. Liska, S.M. Zakeeruddin, M. Grätzel, *Electrochim. Acta*, 195, 34 (2016).
- [12] M.Y.A. Rahman, A.S. Sulaiman, A.A. Umar, M.M. Salleh, *J. Mater. Sci.: Mater. Electron.*, 28, 1674 (2017).
- [13] L.T. Soo, K.S. Loh, A.B. Mohamad, W.R.W. Daud, W.Y. Wong, *J. Power Sources*, 324, 412 (2016).
- [14] Xue, J. Liu, H. Chen, R. Wang, D. Li, J. Qu, L. Dai, *Angew. Chem. Int. Ed.*, 51, 12124 (2012).
- [15] M.J. Ju, J.C. Kim, H.-J. Choi, I.T. Choi, S.G. Kim, K. Lim, J. Ko, J.-J. Lee, I.-Y. Jeon, J.-B. Baek, H. K. Kim, *ACS Nano*, 6, 5243 (2013).
- [16] Z. Wang, P. Li, Y. Chen, J. He, J. Liu, W. Zhang, Y. Li, *J. Power Sources*, 263, 246 (2014).
- [17] M.I.A. Umar, C.C. Yap, R. Awang, A.A. Umar, M.M. Salleh, M. Yahaya, *Mater. Lett.*, 106, 200 (2013).
- [18] L. Roza, A.A. Umar, M.Y.A. Rahman, M.M. Salleh, *Adv. Mater. Res.*, 364, 393 (2012).
- [19] H. Choi, H. Kim, S. Hwang, W. Choi, M. Jeon, *Sol. Energy Mater. Sol. Cells*, 95, 323 (2011).

